Cell, Vol. 119, 121–135, October 1, 2004, Copyright ©2004 by Cell Press

Defects in Adaptive Energy Metabolism with CNS-Linked Hyperactivity in *PGC-1α* Null Mice

Jiandie Lin,[1] Pei-Hsuan Wu,[1] Paul T. Tarr,[1,9] Katrin S. Lindenberg,[2] Julie St-Pierre,[1] Chen-yu Zhang,[3] Vamsi K. Mootha,[4] Sibylle Jäger,[1] Claudia R. Vianna,[3] Richard M. Reznick,[5] Libin Cui,[2] Monia Manieri,[6] Mi X. Donovan,[7] Zhidan Wu,[1,10] Marcus P. Cooper,[1] Melina C. Fan,[1] Lindsay M. Rohas,[1] Ann Marie Zavacki,[8] Saverio Cinti,[6] Gerald I. Shulman,[5] Bradford B. Lowell,[3] Dimitri Krainc,[2] and Bruce M. Spiegelman[1,*]

[1]Dana-Farber Cancer Institute and Department of Cell Biology Harvard Medical School Boston, Massachusetts 02115

[2]Department of Neurology Massachusetts General Hospital Harvard Medical School Mass General Institute for Neurodegeneration Charlestown, Massachusetts 02129

[3]Department of Medicine Division of Endocrinology Beth Israel Deaconess Medical Center and Harvard Medical School Boston, Massachusetts 02215

[4]Whitehead Institute/MIT Center for Genome Research Massachusetts Institute of Technology Cambridge, Massachusetts 02139

[5]Department of Internal Medicine and Cellular and Molecular Physiology Howard Hughes Medical Institute Yale University School of Medicine New Haven, Connecticut 06520

[6]Institute of Normal Human Morphology Faculty of Medicine University of Ancona Ancona 60020 Italy

[7]Department of Medicine Division of Rheumatology Immunology and Allergy

[8]Thyroid Section Division of Endocrinology Diabetes and Hypertension Brigham and Women's Hospital and Harvard Medical School Boston, Massachusetts 02115

Summary

PGC-1α is a coactivator of nuclear receptors and other transcription factors that regulates several metabolic processes, including mitochondrial biogenesis and respiration, hepatic gluconeogenesis, and muscle fiber-type switching. We show here that, while hepatocytes lacking PGC-1α are defective in the program of hormone-stimulated gluconeogenesis, the mice have constitutively activated gluconeogenic gene expression that is completely insensitive to normal feeding controls. C/EBPβ is elevated in the livers of these mice and activates the gluconeogenic genes in a PGC-1α-independent manner. Despite having reduced mitochondrial function, PGC-1α null mice are paradoxically lean and resistant to diet-induced obesity. This is largely due to a profound hyperactivity displayed by the null animals and is associated with lesions in the striatal region of the brain that controls movement. These data illustrate a central role for PGC-1α in the control of energy metabolism but also reveal novel systemic compensatory mechanisms and pathogenic effects of impaired energy homeostasis.

Introduction

Obesity and related metabolic disorders have become leading causes of adult morbidity and mortality worldwide (Zimmet et al., 2001). The profound metabolic dysregulation of this disease is characterized by a cluster of disorders in energy metabolism, including Type 2 diabetes, hyperlipidemia, hypertension, and increased risk for cardiovascular disease (Ginsberg, 2000; Lieberman, 2003). In contrast to Type 1 diabetes, which is caused by autoimmune destruction of pancreatic β cells that leads to insufficient insulin secretion, Type 2 diabetes typically has insufficient insulin secretion with insulin resistance (Saltiel and Kahn, 2001). Excessive hepatic glucose output through abnormally high levels of glycogenolysis and gluconeogenesis as well as poor glucose uptake into muscle and fat are characteristic of both forms of diabetes (Nordlie et al., 1999). Importantly, suppression of hepatic glucose output is thought to be a key mechanism of action for metformin, a widely prescribed oral medication for Type 2 diabetes (Kirpichnikov et al., 2002; Moller, 2001).

Understanding the regulatory circuits that govern cellular energy and glucose metabolism has been a major focus of research interest in the past decade. Recent studies have implicated transcription coactivators of the PGC-1 family, in particular *PGC-1α* and *PGC-1β*, as important regulators of mitochondrial biogenesis and cellular respiration in several cell types (Kelly and Scarpulla, 2004; Puigserver and Spiegelman, 2003). Notably, the expression of *PGC-1α* has been found to be dysregulated in diabetic liver and skeletal muscle, tissues critical for maintaining normal blood glucose levels, while *PGC-1β* mRNA levels are also lowered in diabetic muscle (Mootha et al., 2003; Patti et al., 2003; Yoon et al., 2001). PGC-1α was initially identified as a cold-inducible coactivator for PPARγ in brown fat (Puigserver et al., 1998). Subsequent studies revealed that PGC-1α is able to bind to and augment transcriptional activities of many

*Correspondence: bruce_spiegelman@dfci.harvard.edu

[9]Present address: Department of Biological Chemistry, School of Medicine, University of California, Los Angeles, Los Angeles, California 90095.

[10]Present address: Novartis Institute for Biomedical Research, Cambridge, Massachusetts 02139.

nuclear receptors and several other transcription factors outside the nuclear receptor superfamily. Adenoviral-mediated or transgenic expression of PGC-1α in cultured cells and in vivo leads to activation of mitochondrial biogenesis and increases in cellular respiration (Lehman et al., 2000; Lin et al., 2002b; St-Pierre et al., 2003; Wu et al., 1999). Consistent with a regulatory role in the cellular adaptations to increased energy requirements, the expression of PGC-1α itself is highly regulated in response to nutritional and environmental stimuli. For example, PGC-1α mRNA is strongly induced in brown fat by cold exposure and in skeletal muscle following bouts of physical activity (Baar et al., 2002; Goto et al., 2000; Puigserver et al., 1998). Increased PGC-1α levels in these tissues lead to enhanced mitochondrial electron transport activities that enable cells to meet rising energy demands, such as during adaptive thermogenesis in brown fat and contraction in muscle.

In addition to its role in mitochondrial biology, PGC-1α also regulates several key metabolic programs that go beyond simple mitochondrial biogenesis and oxidative phosphorylation. For example, PGC-1α drives expression of myofibrillar proteins characteristic of slow-twitch muscle fibers when expressed in fast-twitch muscle beds of transgenic mice (Lin et al., 2002b). In the liver, PGC-1α mRNA level is rapidly induced following short-term fasting (Yoon et al., 2001). Adenoviral-mediated expression of PGC-1α in cultured primary hepatocytes and in live rats leads to activation of the entire program of gluconeogenesis and increased glucose production (Yoon et al., 2001). In all of these cases, PGC-1α interacts with cell-selective transcription factors to execute these tissue-specific functions, such as MEF2c in skeletal muscle and HNF4α and FOXO1 in the liver. The activities of PGC-1β have been studied far less, but it appears to share some but not all of these activities of PGC-1α (Lin et al., 2002a, 2003; St-Pierre et al., 2003). PGC-1β induces mitochondrial biogenesis in several cell types and also increases the expression of genes associated with fatty acid oxidation in cultured liver cells or the livers of rats. However, PGC-1β has minimal activity in the induction of gluconeogenic genes, indicating that these two coactivators control overlapping but distinct metabolic programs (Lin et al., 2003).

To date, all of the remarkable and diverse activities of PGC-1α have been investigated using gain-of-function approaches, in either cultured cells, virally transduced animals, or transgenic mice. In this report, we investigated the maintenance of glucose and energy homeostasis in mice deficient in PGC-1α during fasting and feeding and in diet-induced obesity. Our studies demonstrate a critical role for PGC-1α in the control of cellular energy metabolism in several tissues; these studies also reveal unexpected systemic compensatory mechanisms and pathogenesis in the absence of PGC-1α.

Results

Generation of *PGC-1α*$^{-/-}$ mice

To generate mouse strains deficient in PGC-1α by homologous recombination, a targeting plasmid was constructed flanking exons 3 to 5 of the *PGC-1α* gene with loxP sites (see Supplemental Figure S1A at http://www.cell.com/cgi/content/full/119/1/121/DC1/). These three exons encode a highly conserved region in PGC-1α, including the LXXLL motif that mediates its interaction with many nuclear receptors. We generated *PGC-1α*$^{+/-}$ mice through transgenic expression of cre recombinase under the control of ZP3 promoter, which is transiently activated during oocyte development (Lewandoski et al., 1997). *PGC-1α*$^{-/-}$ mice were obtained from offspring of heterozygous breeding pairs. Homologous recombination and cre-mediated excision events were confirmed by hybridization and PCR analysis of genomic DNA isolated from *PGC-1α*$^{+/+}$, *PGC-1α*$^{+/-}$, and *PGC-1α*$^{-/-}$ mice (see Supplemental Figures S1B–S1D on the *Cell* web site). Analysis of PGC-1α expression revealed that its mRNA was absent in skeletal muscle and liver from *PGC-1α*$^{-/-}$ mice and reduced to approximately 50% in *PGC-1α*$^{+/-}$ mice, as revealed by RNA hybridization and real-time PCR analysis (Figure 1A and data not shown). As expected, no PGC-1α protein was detected in the nuclear extract prepared from *PGC-1α*$^{-/-}$ brown fat (Figure 1B).

Pups lacking PGC-1α were born at the expected Mendelian ratio, suggesting that PGC-1α is dispensable for embryonic development. However, only half of *PGC-1α*$^{-/-}$ pups survive early postnatal period and grow into adults (Supplemental Table S1). *PGC-1α*$^{-/-}$ mice weigh approximately 10%–15% less than the *PGC-1α*$^{+/+}$ and *PGC-1α*$^{+/-}$ littermates at 2 months of age and are fertile. Hematoxylin/eosin (H&E) staining of tissue sections revealed normal histology in several tissues, including heart, skeletal muscle, pancreas, and liver (Figures 1C and 1D and data not shown). In contrast, *PGC-1α*$^{-/-}$ brown fat appeared abnormal, with abundant accumulation of large lipid droplets (Figures 1E and 1F), a feature commonly associated with impaired thermogenic function. Electron microscopy studies revealed no obvious changes in the abundance and morphology of mitochondria in brown fat and liver (data not shown). Measurement of plasma and liver lipid levels shows no significant difference between wild-type (wt) and PGC-1α null mice in the fed state, while the triglyceride content is lower in the liver of null mice in the fasted state (Supplemental Table S2).

A Critical Role for PGC-1α in Hormone-Induced Gluconeogenesis

PGC-1α has been shown to influence glucose metabolism in muscle and liver. The expression of PGC-1α itself is induced in liver in response to fasting, a metabolic state characterized by active glycogenolysis, gluconeogenesis, and fatty acid β oxidation (Aoki, 1981). To examine the requirement for PGC-1α in the regulation of glucose metabolism, we measured blood glucose and insulin levels in mice under various nutritional states. There is no difference in plasma glucose levels in *PGC-1α*$^{+/+}$, *PGC-1α*$^{+/-}$, and *PGC-1α*$^{-/-}$ mice when food is provided ad libitum (Figure 2A). Mice deficient in PGC-1α, however, develop mild hypoglycemia after 24 hr of fasting. Examination of blood insulin levels revealed that, although *PGC-1α*$^{-/-}$ mice are able to maintain euglycemia in the fed state, they do so with reduced circulating insulin concentrations (Figure 2B). In contrast, no reduction in insulin levels was observed in *PGC-1α*$^{-/-}$ mice in the fasted state. Blood glucose levels tend to be lower in the *PGC-1α*$^{-/-}$ mice after prolonged fasting

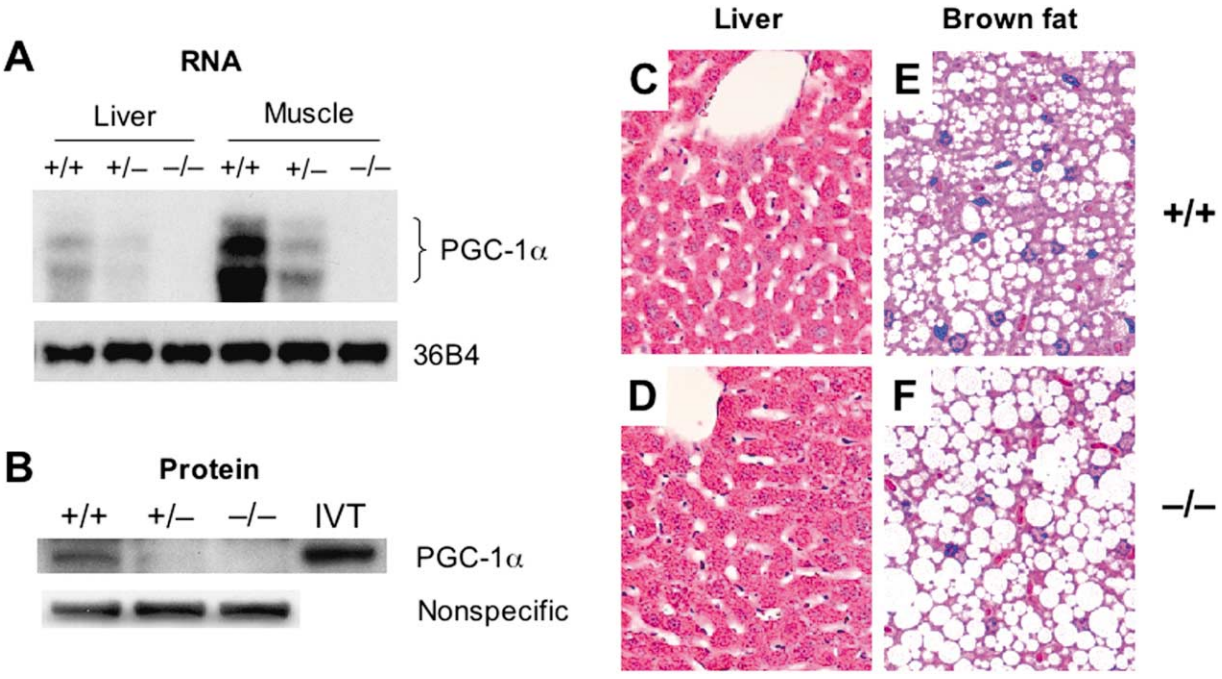

Figure 1. Generation of *PGC-1α*-Deficient Mice

(A) Hybridization analysis of PGC-1α mRNA in liver and skeletal muscle using a probe spanning exons 3 to 5 of *PGC-1α*. Hybridization with a probe specific for ribosomal protein 36B4 was included as a loading control.

(B) Immunoblotting of PGC-1α protein. Lysates containing in vitro-translated PGC-1α were used as a positive control. Note the absence of PGC-1α protein in brown fat extracts from *PGC-1α*$^{-/-}$ mice.

(C and D) H&E staining of paraffin-embedded liver sections.

(E and F) H&E staining of plastic-embedded brown fat sections.

(48 hr), although the difference does not reach statistical significance.

PGC-1α has been shown to control the expression of genes involved in mitochondrial fatty acid β oxidation and oxidative phosphorylation in various cell types, including hepatocytes. Proper mitochondrial respiration is necessary to generate the ATP that supports the enzymatic function of the gluconeogenic pathway. To determine the effects of PGC-1α deficiency on mitochondrial respiration, we next used an oxygen electrode to measure O_2 consumption in isolated hepatocytes. Total O_2 consumption rate is reduced 17% in *PGC-1α*$^{-/-}$ hepatocytes compared to wt controls (Figure 2C). Respiration due to mitochondrial proton leak is also reduced approximately 20% in the PGC-1α-deficient hepatocytes (Figure 2C). These data illustrate that mitochondrial function is impaired in the hepatocytes from *PGC-1α*$^{-/-}$ mice.

Hepatic gluconeogenesis is of major importance in the fasted state (Hanson and Reshef, 1997; Pilkis and Granner, 1992) and is controlled by PGC-1α in gain-of-function experiments (Herzig et al., 2001; Yoon et al., 2001). The induction of PGC-1α and gluconeogenic genes such as *phosphoenolpyruvate carboxykinase (PEPCK)* and *glucose-6-phosphatase (G6Pase)* are mediated by a rise in the circulating concentrations of counterregulatory hormones, such as glucagon and glucocorticoids, and a fall in insulin levels. To determine whether PGC-1α is essential for expression of this program, we isolated primary hepatocytes from *PGC-1α*$^{+/+}$ and *PGC-1α*$^{-/-}$ mice and examined the expression of the *PEPCK* and *G6Pase* genes in response to hormonal treatments. Basal levels of *PEPCK* and *G6Pase* mRNA were similar in *PGC-1α*$^{+/+}$ and *PGC-1α*$^{-/-}$ hepatocytes, as revealed by RNA hybridization and quantitative real-time PCR analysis (Figure 2D and data not shown). Following treatments with glucocorticoid and forskolin, *PGC-1α*$^{+/+}$ hepatocytes exhibit a robust and dose-dependent increase in *PEPCK* and *G6Pase* mRNA (Figure 2D). In contrast, the induction of *PEPCK* and *G6Pase* mRNA expression is greatly diminished in hepatocytes isolated from *PGC-1α*$^{-/-}$ mice at all treatment conditions examined. These results clearly demonstrate that PGC-1α is an essential mediator of transcriptional activation of gluconeogenic genes in response to hormonal stimulation in isolated hepatocytes.

To determine whether PGC-1α is necessary for gluconeogenesis in vivo, we examined blood glucose levels in mice following intraperitoneal injection of pyruvate, an important substrate for this pathway. Consistent with defects in gluconeogenic gene expression and mitochondrial function in the *PGC-1α*$^{-/-}$ hepatocytes, mice lacking PGC-1α have greatly reduced ability to convert pyruvate into glucose as compared to wt littermates (Figure 2E).

Constitutive Activation of the Hepatic Gluconeogenic Program In Vivo in the Absence of PGC-1α

The experiments in primary hepatocytes strongly suggest that impaired mitochondrial function and a reduced hepatic gluconeogenic program may be responsible for fasting hypoglycemia in *PGC-1α*$^{-/-}$ mice. We next ex-

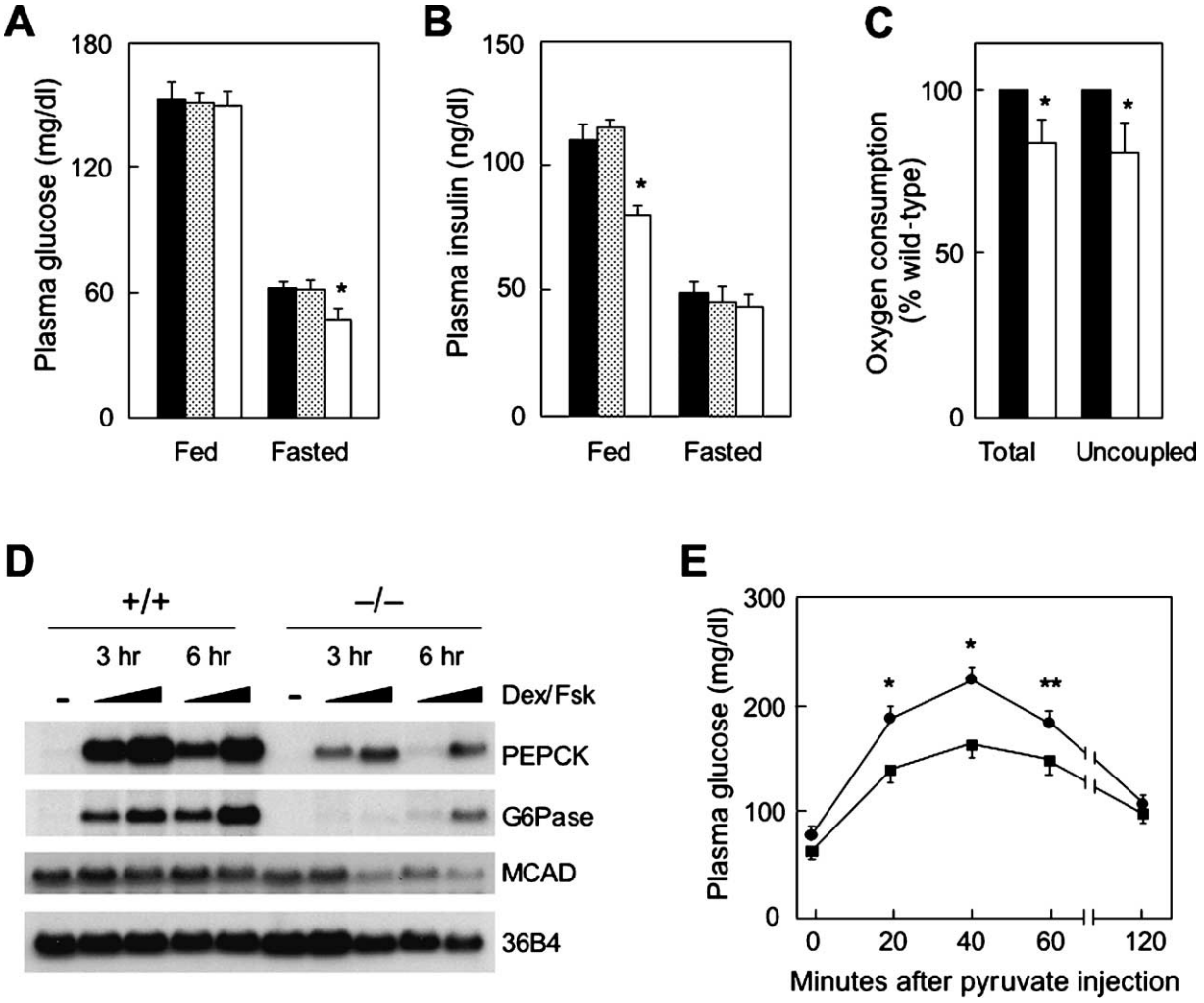

Figure 2. Impaired Glucose Homeostasis and Hepatic Energy Metabolism in the Absence of PGC-1α

(A) Plasma glucose levels in *PGC-1*$\alpha^{+/+}$ (filled box), *PGC-1*$\alpha^{+/-}$ (dotted box), and *PGC-1*$\alpha^{-/-}$ (open box) in the fed and fasted (24 hr) states. *$p = 0.0007$.

(B) Plasma insulin concentrations in the same group of mice used in (A). *$p = 0.005$.

(C) Total and uncoupled respiration in wt (+/+) and PGC-1α-deficient (−/−) hepatocytes. O_2 consumption rate was measured as described in Experimental Procedures; the rate of *PGC-1*$\alpha^{-/-}$ cells is normalized to wt values measured on the same day. *$p < 0.02$. Data in (A)–(C) represent mean ± SEM.

(D) Defective hormone-induced gluconeogenic gene expression in hepatocytes lacking PGC-1α. Primary hepatocytes were isolated from *PGC-1*$\alpha^{+/+}$ and *PGC-1*$\alpha^{-/-}$ mice and treated with 0.2 μM or 1.0 μM of a combination of forskolin and dex for 3 or 6 hr before RNA isolation and hybridization. Hybridization for ribosomal protein 36B4 mRNA was included as a loading control.

(E) Pyruvate tolerance test. Three-month-old male mice were fasted overnight before receiving intraperitoneal (i.p.) injection of a pyruvate solution, as described in Experimental Procedures. *$p < 0.0002$; **$p < 0.02$.

amined the nutritional regulation of *PEPCK* and *G6Pase* genes under fed and fasted states in the mice. As expected, wt mice activate multiple adaptive metabolic changes in response to fasting (Figure 3A), as shown by increased expression of gluconeogenic genes and those involved in fatty acid oxidation (*MCAD*), ketone body synthesis (mitochondrial *HMG-CoA synthase*), and bile acid synthesis (*Cyp7a1*) (Rhee et al., 2003; Shin et al., 2003). Surprisingly, the expression of *PEPCK*, *G6Pase*, *HMG-CoA synthase*, and *MCAD* is similar in *PGC-1*$\alpha^{+/+}$ and *PGC-1*$\alpha^{-/-}$ liver in the fasted state (Figure 3A). More unexpectedly, the mRNA levels of *PEPCK*, *G6Pase*, and *HMG-CoA synthase* are greatly elevated in *PGC-1*$\alpha^{-/-}$ mouse liver under *fed* conditions (Figure 3A). Notably, expression of *G6Pase* in the fed state is near the level that is usually seen in fasted liver. These results indicate that, although PGC-1α is not required for the expression of gluconeogenic and ketogenic genes, this coactivator is essential for proper nutritional regulation of this response. Since basal levels of *PEPCK* and *G6Pase* expression are similar in untreated primary hepatocytes in the presence or absence of PGC-1α (Figure 2D), this suggests very strongly that systemic signals are probably responsible for the constitutive activation of these genes under fed conditions in mice lacking PGC-1α.

The aberrant activation of *PEPCK* and *G6Pase* expres-

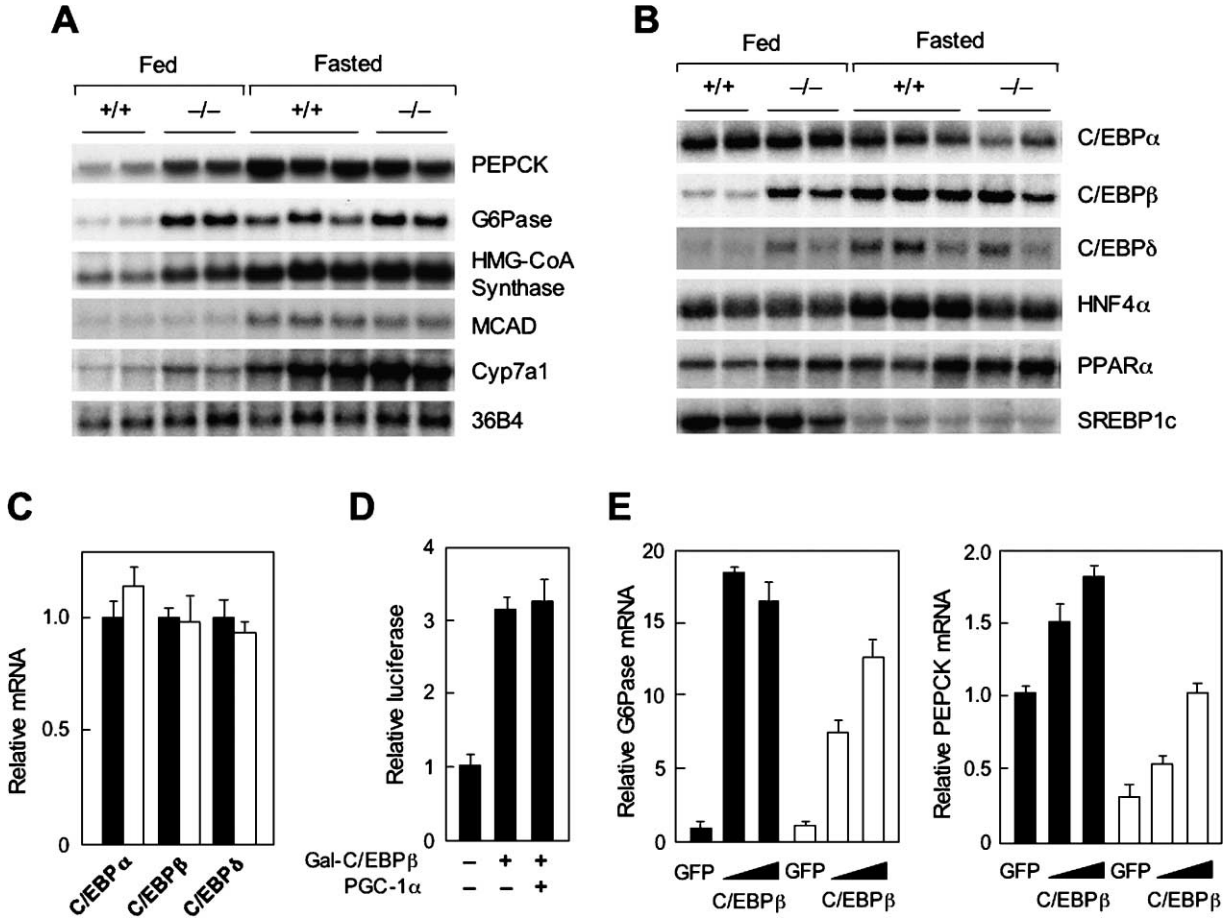

Figure 3. Constitutive Activation of the Gluconeogenic Program in PGC-1α-Deficient Liver

(A) Hybridization analysis of mRNAs for metabolic genes in the fed and fasted liver. Three-month-old male mice were fed ad libitum or fasted for 24 hr before harvesting tissues for mRNA analysis.

(B) Expression of mRNAs for transcription factors that regulate hepatic metabolism. Note the dramatic induction of C/EBPβ mRNA in fed *PGC-1*$\alpha^{-/-}$ liver compared to wt liver.

(C) Real-time PCR analysis of mRNA levels for the C/EBP family members.

(D) PGC-1α does not coactivate C/EBPβ. H2.35 hepatoma cells were transiently transfected with a UAS-luciferase reporter with Gal4-DBD-C/EBPβ in the presence or absence of PGC-1α. Luciferase activity was measured 30 hr following transfection.

(E) Induction of endogenous gluconeogenic genes by C/EBPβ in primary hepatocytes. Primary hepatocytes were isolated from *PGC-1*$\alpha^{+/+}$ (filled box) and *PGC-1*$\alpha^{-/-}$ (open box) mouse liver and infected with adenoviruses expressing GFP or C/EBPβ. Total RNA were harvested following 3 hr of treatments with 0.2 μM forskolin and 0.1 μM dex. Relative abundance of *G6Pase* and *PEPCK* mRNA was examined by real-time PCR followed by normalization to 18S ribosomal RNA.

sion is likely due to dysregulation of one or more transcription factors that can regulate the *PEPCK* and *G6Pase* genes in the absence of PGC-1α. To assess this possibility, we examined mRNA levels of several transcription factors known to have at least some connection with this process. As shown in Figure 3B, the expression of HNF4α and PPARα, key regulators of hepatic metabolism in the fasted state, was comparable in *PGC-1*$\alpha^{+/+}$ and *PGC-1*$\alpha^{-/-}$ liver in the fed state, although the induction of HNF4α in response to fasting is blunted in the absence of PGC-1α. The mRNA levels for FOXO1 and GR remain unchanged between genotypes in both fed and fasted states (data not shown). As expected, the expression of sterol response element binding protein 1c (SREBP1c), a central regulator of hepatic lipogenesis (Horton et al., 2002), is suppressed in response to fasting in both *PGC-1*$\alpha^{+/+}$ and *PGC-1*$\alpha^{-/-}$ mice. This indicates that, although the expression of gluconeogenic and ketogenic genes is dysregulated in the absence of PGC-1α, the nutritional regulation of *SREBP1c* is still intact. In contrast, there is a striking increase in the abundance of C/EBPβ mRNA in *PGC-1*$\alpha^{-/-}$ mouse liver, precisely mirroring the aberrant expression of *PEPCK* and *G6Pase* in the fed state (Figure 3A). C/EBPβ is normally induced in the fasted state in wt animals but is abnormally activated in the fed state in the null mice. C/EBPδ is also induced in the fed liver lacking PGC-1α, while C/EBPα is expressed normally with respect to *PGC-1*α genotypes. The aberrant induction of C/EBPβ and C/EBPδ, however, is absent when PGC-1α-deficient hepatocytes are grown in cell culture, suggesting that systemic signals are likely responsible for their in-

creased expression (Figure 3C). These results suggest that altered C/EBP transcription factor activities, particularly C/EBPβ, may potentially play a role in the constitutive activation of gluconeogenic gene expression seen in the PGC-1α-deficient mouse liver.

PGC-1α-Independent Activation of Gluconeogenic Genes by C/EBPβ

C/EBPβ is a transcription factor that belongs to the basic leucine zipper family and has been shown to modulate the activity of the transfected *PEPCK* promoter in response to gluconeogenic hormones (Croniger et al., 1998; Park et al., 1993; Roesler, 2001). Pups lacking *C/EBP*β develop severe hypoglycemia, and half of them died shortly after birth due to a failure to activate hepatic gluconeogenic gene expression and glucose production (Croniger et al., 1997; Liu et al., 1999). The effects of C/EBPβ on the endogenous gluconeogenic genes have not been studied. Moreover, a functional interaction between C/EBPβ and PGC-1α has not been examined to date. As shown in Figure 3D, PGC-1α does not coactivate C/EBPβ in transient transfection assays. We next ask whether C/EBPβ could modulate expression of endogenous genes of gluconeogenesis and whether it could do so in the absence of PGC-1α. Primary hepatocytes were isolated from wt and PGC-1α-deficient mice, infected with a recombinant adenovirus expressing a control GFP protein or C/EBPβ, and examined for the expression of *PEPCK* and *G6Pase*. As shown in Figure 3E, adenoviral-mediated expression of C/EBPβ activates the transcription of the *G6Pase* gene approximately 17-fold in wt hepatocytes. *PEPCK* mRNA level is also elevated 1.8-fold in response to ectopic C/EBPβ expression. Importantly, induction of gluconeogenic gene expression by C/EBPβ was also observed in the *PGC-1*$\alpha^{-/-}$ cells with a 12-fold increase in *G6Pase* mRNA and approximately 3-fold induction of *PEPCK* mRNA. The absolute levels of these mRNAs are somewhat higher in hepatocytes with an intact *PGC-1*α gene. These results demonstrate that C/EBPβ is able to turn on gluconeogenic gene expression in a PGC-1α-independent manner and strongly suggest that elevated C/EBPβ in *PGC-1*$\alpha^{-/-}$ animals may be at least partially responsible for the inappropriate activation of those gluconeogenic genes in the fed state.

PGC-1$\alpha^{-/-}$ Mice Are Resistant to Diet-Induced Obesity

The well-established role of PGC-1α in stimulating mitochondrial respiration, as well as the reduction of respiration in PGC-1α-deficient hepatocytes (Figure 2C) and abnormal brown fat morphology (Figure 1D), all suggest that the null mice may be prone to the development of obesity due to reduced energy expenditure. To critically assess this, we fed the animals a high-fat diet containing 58% of calories derived from fat. As shown in Figure 4A and as expected, wt mice gain substantial body weight throughout the course of high-fat feeding. In contrast, *PGC-1*$\alpha^{-/-}$ mice are surprisingly *resistant* to diet-induced obesity (Figure 4A). Analysis of body fat content using a dual energy X-ray absorptiometry (DEXA) scanner revealed that *PGC-1*$\alpha^{-/-}$ mice are remarkably leaner (22.6% ± 2.4% body fat, n = 6) than the *PGC-1*$\alpha^{+/+}$ controls (39.8% ± 2.8% body fat, n = 5) after 16 weeks of high-fat feeding (Figures 4B and 4C). In fact, a small but significant decrease in body fat content was observed in *PGC-1*$\alpha^{-/-}$ mice fed a chow diet (Figure 4C). As expected from their obesity, high-fat-fed *PGC-1*$\alpha^{+/+}$ mice developed insulin resistance, as indicated by elevated fasting glucose and insulin concentrations and in vivo insulin tolerance test (Figures 4D and 4E). *PGC-1*$\alpha^{-/-}$ mice, however, display significantly enhanced insulin sensitivity and improved glycemic control in a glucose tolerance test (Figures 4E and 4F) as compared to the control mice. Similar results were seen in *PGC-1*$\alpha^{-/-}$ mice when maintained on a normal rodent chow (data not shown). These data clearly indicate that PGC-1α null mice are resistant to obesity caused by high-fat feeding and are protected from developing insulin resistance and glucose intolerance that ordinarily accompany this obesity.

We next examined the two major arms of energy balance: energy intake as measured by food intake and energy expenditure. Both *PGC-1*$\alpha^{+/+}$ and *PGC-1*$\alpha^{-/-}$ mice show similar food intake at various time points during postnatal development and high-fat feeding (Figure 5A and data not shown). In contrast, energy expenditure, measured as O_2 consumption, is approximately 23% higher in *PGC-1*$\alpha^{-/-}$ mice throughout a 3 day period of metabolic monitoring (Figure 5B). Thus, the resistance to diet-induced obesity in *PGC-1*$\alpha^{-/-}$ mice correlates with a substantial increase in energy expenditure.

Reduced Thermogenic Capacity and Hyperactivity in *PGC-1*$\alpha^{-/-}$ Mice

Two key components of energy expenditure are adaptive thermogenesis and physical activity. To determine whether increased O_2 consumption in *PGC-1*$\alpha^{-/-}$ mice is due to enhanced thermogenesis, we examined the thermogenic capacity of these animals with a standard cold challenge. Resting body temperature is similar between *PGC-1*$\alpha^{+/+}$ and *PGC-1*$\alpha^{-/-}$ mice (Figure 5C, t = 0). We next exposed 6-week-old mice to 4°C and monitored their core body temperature. Both *PGC-1*$\alpha^{+/+}$ and *PGC-1*$\alpha^{-/-}$ mice respond to cold temperature by increasing frequency of shivering. In contrast to wt littermates, which are able to keep body temperature around 36.5°C after an initial drop of approximately 1.5°C, *PGC-1*$\alpha^{-/-}$ mice display striking sensitivity to the cold temperature (Figure 5C). The body temperature of *PGC-1*$\alpha^{-/-}$ mice drops to 33.5°C within 3 hr, and the hypothermia becomes lethal if the exposure of the null mice is extended beyond 6 hr (data not shown). Defense of body temperature in mice is mainly the function of brown adipose tissue, which generates heat due in large part to abundant expression of the mitochondrial uncoupler *UCP1* (Bouillaud et al., 1985; Jacobsson et al., 1985). Analysis of brown fat gene expression revealed that the induction of *UCP1* in the null mice was reduced to approximately 45% of the wt level, while the induction of type 2 iodothyronine deiodinase (*D2*) mRNA was reduced nearly 50% in *PGC-1*$\alpha^{-/-}$ mice compared to controls (Figure 5D). The expression of PGC-1β is unchanged, while mRNAs encoding several enzymes involved in mitochondrial electron transport and fatty acid oxidation are reduced in *PGC-1*$\alpha^{-/-}$ brown fat (Supplemental Figure S2). These

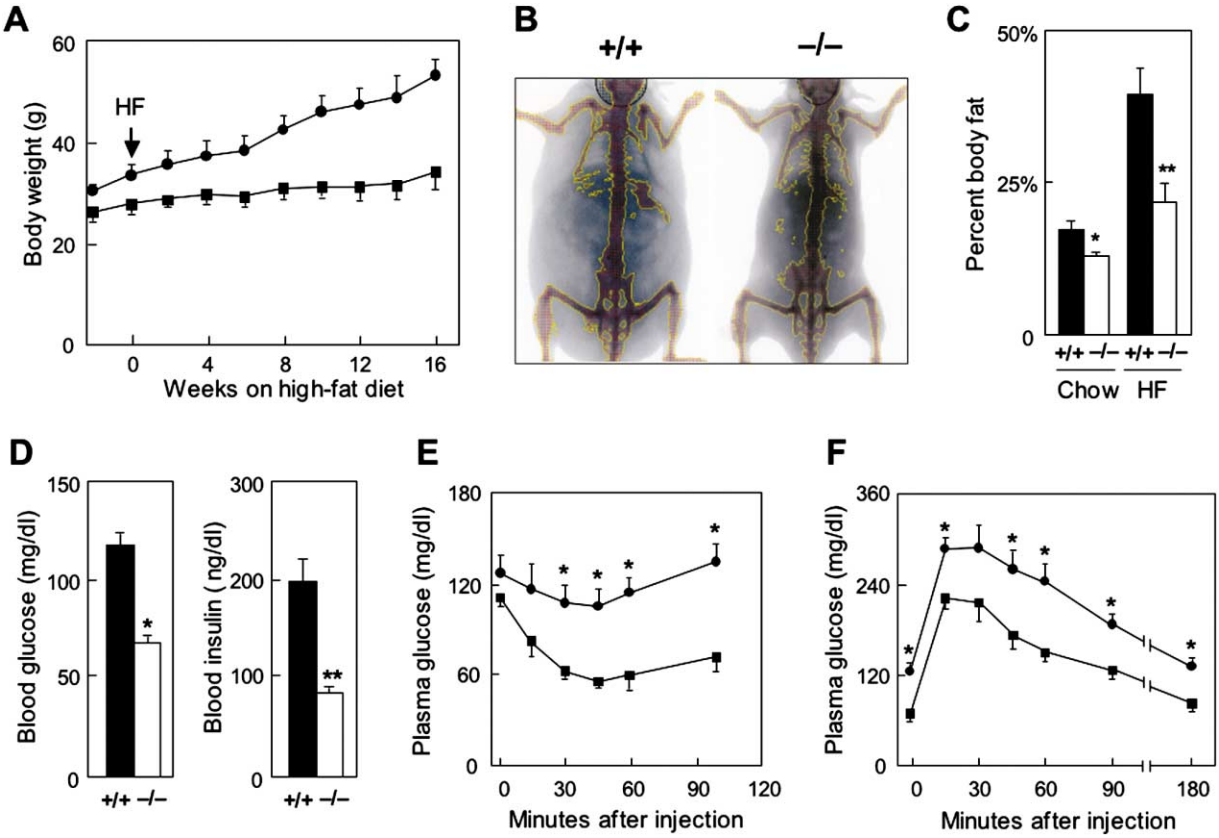

Figure 4. Resistance to Diet-Induced Obesity and Insulin Resistance in *PGC-1*$\alpha^{-/-}$ mice

(A) Body weight of *PGC-1*$\alpha^{+/+}$ (filled circle, n = 6) and *PGC-1*$\alpha^{-/-}$ (filled square, n = 6) mice fed a high-fat diet. Twelve-week-old males were fed a high-fat diet for 16 weeks. Body weight was measured weekly.

(B) Representative DEXA scanning images of *PGC-1*$\alpha^{+/+}$ and *PGC-1*$\alpha^{-/-}$ mice after 12 weeks of high-fat feeding.

(C) Body fat content in *PGC-1*$\alpha^{+/+}$ and *PGC-1*$\alpha^{-/-}$ mice under chow (4-month-old males) or high-fat feeding. Percent body fat was determined by automated analysis of DEXA images with a program supplied by the manufacturer. *p = 0.005; **p = 0.001.

(D) Fasting glucose and insulin levels in high-fat-fed mice. *p = 0.0001; **p = 0.02.

(E) Insulin tolerance test on high-fat-fed *PGC-1*$\alpha^{+/+}$ (filled circle, n = 5) and *PGC-1*$\alpha^{-/-}$ (filled square, n = 5) mice. *p < 0.004.

(F) Glucose tolerance test in high-fat-fed mice following an overnight fast. *p < 0.02. Insulin and glucose tolerance tests were performed as described in Experimental Procedures. Data in (A) and (C)–(F) represent mean ± SEM.

data indicate that the increased energy expenditure in the *PGC-1*$\alpha^{-/-}$ mice is not due to increased thermogenesis in these animals; on the contrary, the mice are hypothermic when challenged.

Skeletal muscle is a major tissue involved in energy expenditure in vivo. To determine whether PGC-1α is also required for normal mitochondrial function in skeletal muscle, we next examined mitochondrial gene expression in quadriceps muscle from wt and PGC-1α null mice. MRNA levels for a large number of genes involved in fatty acid oxidation and mitochondrial function are reduced 30%–60% in *PGC-1*$\alpha^{-/-}$ mice, including those involved in intracellular fatty acid trafficking, the Kreb's cycle, electron transport (*Ndufb5* and *Cox7a1*), ATP synthesis (*Atp5j*), and mitochondrial protein translation (Figure 5E and data not shown). Interestingly, the expression of ERRα, a direct target of PGC-1α and an important mediator of PGC-1α action, is also reduced in the absence of PGC-1α, while the *PGC-1*β mRNA level remains largely unchanged (Figure 5E).

Impaired mitochondrial energy metabolism might be expected to negatively affect ATP/AMP ratios. Consistent with this, AMP-activated protein kinase (AMPK), a key component of cellular energy-sensing pathways (Carling, 2004), is strongly activated in PGC-1α-deficient skeletal muscle. The levels of phosphorylated AMPK and acetyl-CoA carboxylase (ACC), a known substrate for activated AMPK, are significantly increased in *PGC-1*$\alpha^{-/-}$ muscle (Figure 5F). These data clearly indicate that PGC-1α is essential for normal mitochondrial gene expression and energy metabolism in skeletal muscle.

The lack of an increase in thermogenesis or mitochondrial gene expression in the mutant animals suggested that the higher metabolic rate in PGC-1α-deficient mice might be caused by altered levels of physical activity. To assess this possibility, we monitored and quantitated the frequency of animal movements using the Comprehensive Lab Animal Monitoring System (CLAMS), which is capable of simultaneously recording whole-body O_2 consumption and physical activity. As shown in Figures 6A and 6B, a higher O_2 consumption rate in *PGC-1*$\alpha^{-/-}$ mice is accompanied by profound hyperactivity, as indicated by increased physical movement. PGC-1α-deficient mice are hypermetabolic and hyperactive com-

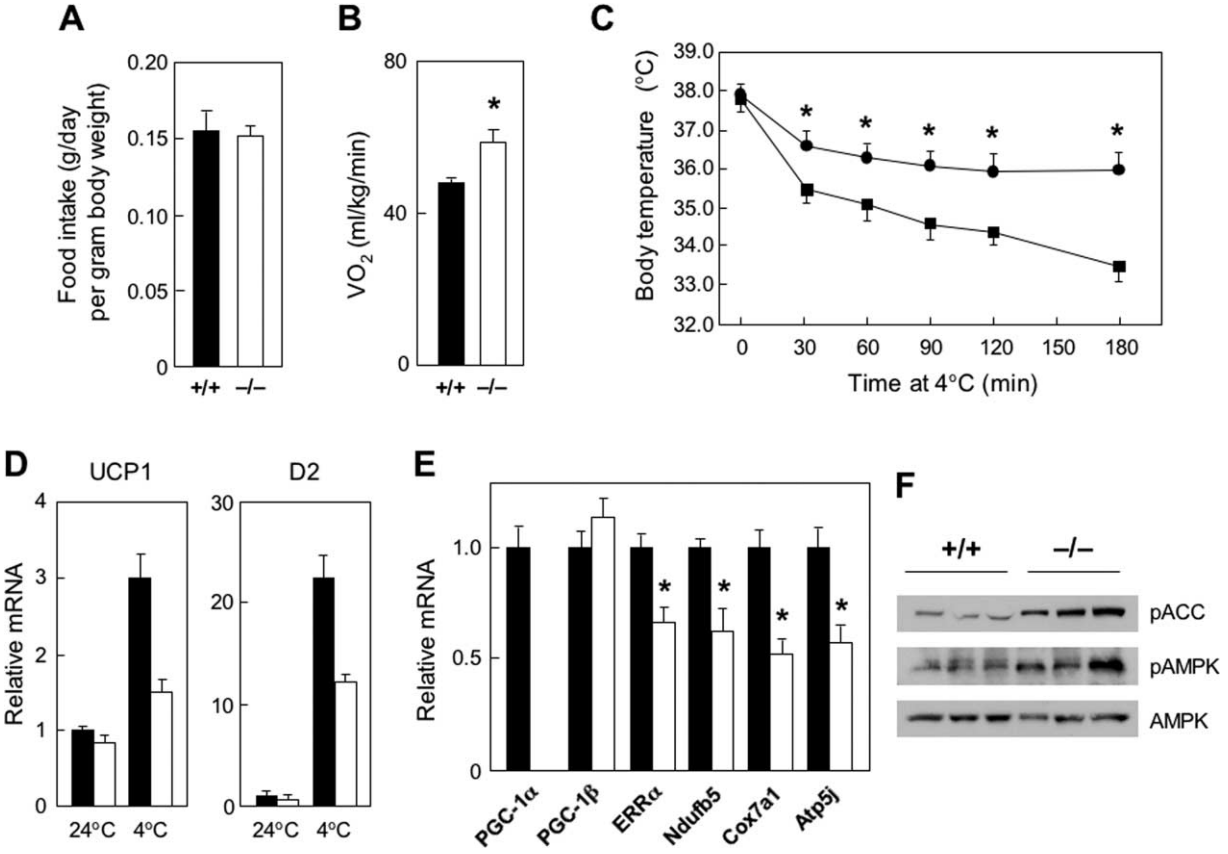

Figure 5. Analysis of Whole-Body Energy Balance and Thermogenesis in *PGC-1*$\alpha^{-/-}$ Mice

(A) Food intake was measured in a 2 day period and normalized to body weight.

(B) Whole-body O_2 consumption in *PGC-1*$\alpha^{+/+}$ (n = 5) and *PGC-1*$\alpha^{-/-}$ (n = 5) mice as monitored by CLAMS. Shown is the averaged value over 2 days and 3 nights. *$p < 0.006$.

(C) Body temperature of 6- to 7-week-old *PGC-1*$\alpha^{+/+}$ (circle, n = 6) and *PGC-1*$\alpha^{-/-}$ (square, n = 6) mice exposed to cold temperature (4°C). Body temperature was measured with a rectal thermometer. *$p < 0.008$. Data in (B) and (C) represent mean ± SEM.

(D) Gene expression in brown fat analyzed by quantitative real-time PCR. Intrascapular brown fat was dissected from *PGC-1*$\alpha^{+/+}$ (filled box) and *PGC-1*$\alpha^{-/-}$ (open box) mice maintained at 24°C or after 5 hr of cold exposure at 4°C. Primers specific for *18S* ribosomal RNA were used for normalization.

(E) Analysis of skeletal muscle gene expression in wt (filled box) and PGC-1α-deficient (open box) mice by quantitative real-time PCR. Quadriceps muscle was dissected from 4-month-old male mice and frozen at −80°C before RNA isolation and analysis. Primers specific for *18S* ribosomal RNA were used for normalization.

(F) Activation of AMPK in *PGC-1*$\alpha^{-/-}$ skeletal muscle. Tissue extracts were prepared from wt or PGC-1α null quadriceps muscle and analyzed by immunoblotting using antibodies specific for phosphorylated AMPK (pAMPK) and ACC (pACC) or an antibody that reacts with both phosphorylated and nonphosphorylated forms of AMPK.

pared to wt controls both during daytime and at night. In fact, the PGC-1α null mice displayed a 40% increase in the frequency of random movements during the monitoring period (Figure 6C). These results strongly suggest that much of the increase in energy expenditure seen in *PGC-1*$\alpha^{-/-}$ mice is due to the hyperactivity displayed by the null animals.

Striatal Degeneration in PGC-1α Null Mouse Brain

Hyperactivity in *PGC-1*$\alpha^{-/-}$ mice could result from altered circulating hormones and/or signals that originated from the central nervous system. Measurements of several hormones known to influence animal movement, including thyroid hormone and catecholamines, showed no significant alterations (Supplemental Table S3). Besides a simple increase in total movement, we observed that PGC-1α null mice display behavioral changes that are characteristic of certain neurological disorders, including stimulus-induced myoclonus, exaggerated startle responses, dystonic posturing, and frequent limb clasping (Figure 6D). These findings are suggestive of lesions in the striatum, the brain area that is affected in certain neurodegenerative diseases characterized by disorders of movement, including Huntington's disease (HD).

We assessed neuropathology in the *PGC-1*$\alpha^{-/-}$ mouse brain by histological analysis. The overall brain anatomy appeared similar in the *PGC-1*$\alpha^{+/+}$ and *PGC-1*$\alpha^{-/-}$ mice. However, a striking spongiform pattern of lesions was found predominantly in the striatum of 3-month-old *PGC-1*$\alpha^{-/-}$ mice (Figure 7). The number and size of lesions decrease from the dorsal to the ventral side and also from the lateral to the medial parts of the striatum. Occasionally, much smaller and less abundant lesions were also found in the cortex, especially in cortical layer V/VI of the motor cortex, nucleus

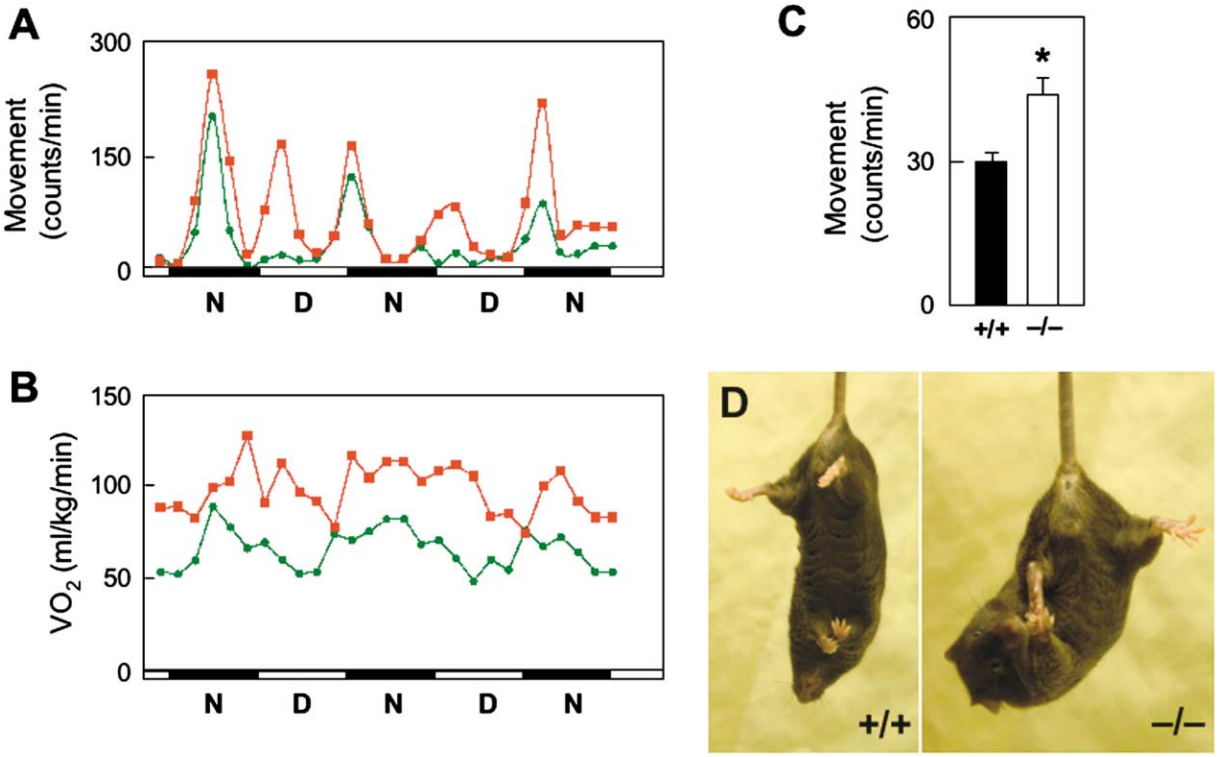

Figure 6. Hyperactivity and Limb Clasping in *PGC-1*$\alpha^{-/-}$ Mice

(A) Representative trace of movement monitoring for *PGC-1*$\alpha^{+/+}$ (green) and *PGC-1*$\alpha^{-/-}$ (red) mice over a period of 3 days.

(B) Representative trace of whole-body O_2 consumption in *PGC-1*$\alpha^{+/+}$ (green) and *PGC-1*$\alpha^{-/-}$ (red) mice. N and D denote night and day periods, respectively.

(C) Physical activity was measured in 3-month-old male mice with CLAMS. Shown is the average movement counts during the monitoring period. *$p < 0.01$.

(D) Limb clasping in *PGC-1*$\alpha^{-/-}$ mice.

accumbens, thalamus, substantia nigra, hippocampus, and the mammalliary body. The spongiform lesions in the striatum were associated with gliosis, as indicated by strong immunoreactivity for glial fibrillary-associated protein (*GFAP*), a hallmark for reactive astrocytes (Figures 7E and 7F). No reactive astrocytes were found in the minor lesions in other brain areas. To determine if the lesions were mainly affecting the white matter, brain sections of *PGC-1*$\alpha^{+/+}$ and *PGC-1*$\alpha^{-/-}$ mice were stained with Luxol fast blue for myelin. As seen in Figures 7A–7D, lesions are predominantly associated with the white matter and rarely with the gray matter. The overall neuronal density appeared similar in wt mice and PGC-1α null mice, although we occasionally observed neurons containing vacuoles in *PGC-1*$\alpha^{-/-}$ mouse brain. Immunostaining using a neurofilament heavy chain (*NF220*) antibody showed a dramatic loss of NF220-positive fibers in the striatum in the absence of PGC-1α (Figures 7G and 7H). In fact, the spongiform lesions appear to arise from the loss of axons in the striatal area in *PGC-1*$\alpha^{-/-}$ mouse brain. These results clearly demonstrate that PGC-1α is required for normal brain function and that loss of PGC-1α leads to neuronal degeneration in specific brain areas, most prominently in the striatum.

PGC-1α has been shown to regulate oxidative metabolism and biological programs associated with increased oxidative capacity in a tissue-specific manner. Analysis of gene expression in the brains of wt and mutant mice by real-time PCR revealed that mRNA levels of many mitochondrial genes are reduced in mutants (Figure 8A). Interestingly, the expression of several brain-specific genes not involving mitochondrial function, including those encoding neurofilament proteins (*NF-H* and *NF-M*), myelin-associated oligodendrocyte basic protein (*MOBP*), and Na^+/K^+ ATPase (*ATP1a2*) is also significantly reduced in the PGC-1α null brain compared to wt controls (Figure 8B). In contrast, mRNA encoding another sodium pump subunit, *ATP1a1*, is not altered. These results suggest that, in addition to its key role in the regulation of mitochondrial gene expression, PGC-1α may also have an important function in the control of neuronal gene expression and function. In fact, primary striatal neurons isolated from *PGC-1*$\alpha^{-/-}$ mouse embryos display a severe impairment in neurite growth (Figures 8C and 8D). Striatal neurons lacking PGC-1α have greatly reduced branches of neurites, whereas wt neurons exhibit robust neurite outgrowth and form an extensive network in culture.

Discussion

PGC-1α has been shown to play several important roles in the metabolism of multiple tissues in response to external stimuli (Kelly and Scarpulla, 2004; Puigserver and Spiegelman, 2003). In this paper, we have analyzed

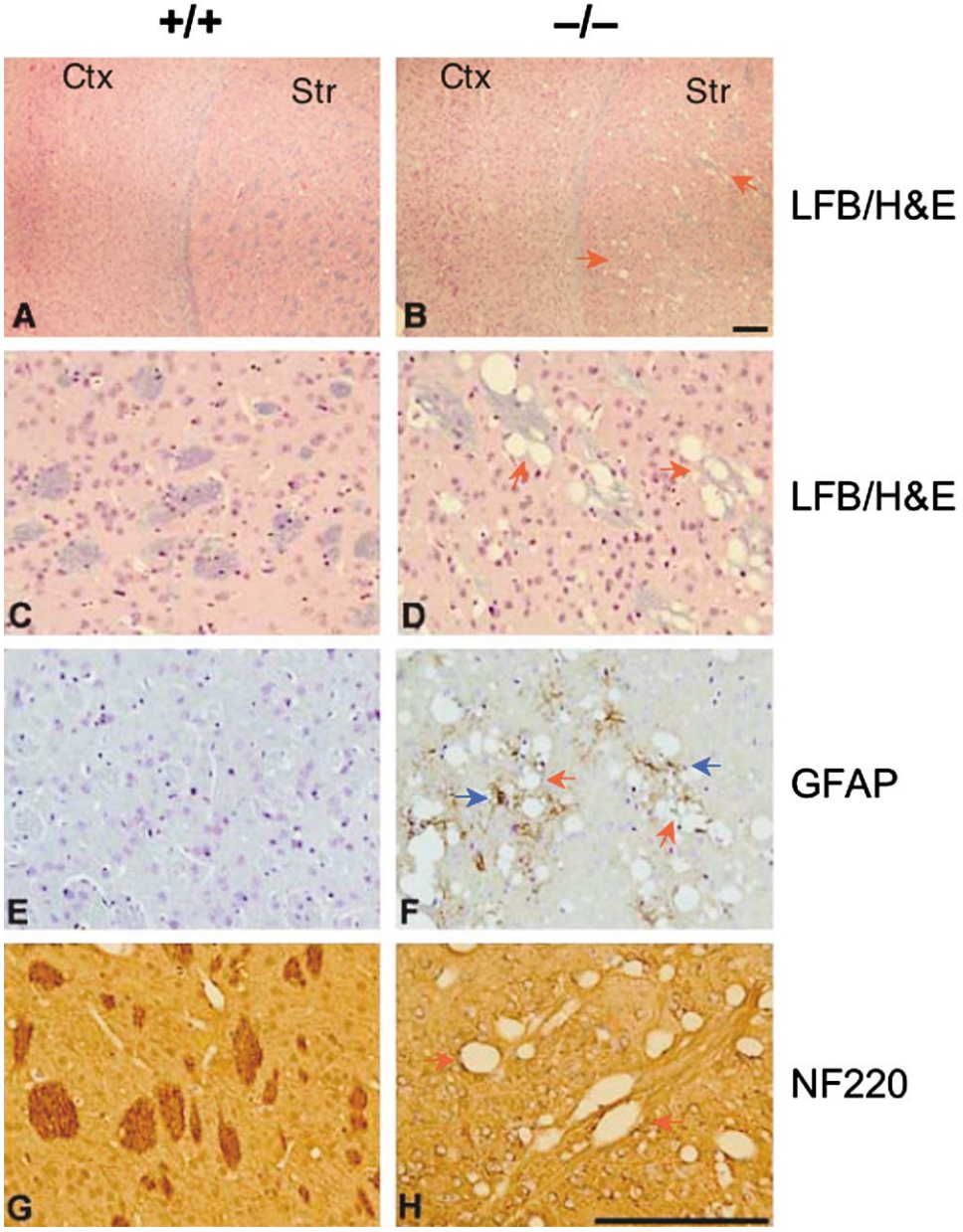

Figure 7. Histological Staining of Brain Sections from Wild-Type and *PGC-1*α Null Mice

(A and B) Low magnification pictures showing cortex (ctx) and striatum (str) of *PGC-1*$\alpha^{+/+}$ mouse brain (A) and PGC-1$\alpha^{-/-}$ mice (B) stained with Luxol fast blue and H&E. Note spongiform pathology predominantly in the striatum of the PGC-1$\alpha^{-/-}$ mouse brain (red arrows). Scale bar, 200 μm.

(C and D) High-magnification pictures of the striatum of wt (C) and PGC-1$\alpha^{-/-}$ brains (D) stained with Luxol fast blue/H&E. Shown are spongiform lesions in the striatum that are predominantly associated with the white matter.

(E and F) Immunohistochemical staining with an anti-GFAP antibody. Note abundant presence of reactive astrocytes (blue arrows) in the striatum of PGC-1$\alpha^{-/-}$ mice (F) but not in wt controls (E).

(G and H) Less striatal neurites are detected in the PGC-1$\alpha^{-/-}$ brain (H) with a neurofilament heavy chain antibody compared to wt striatum (G). Scale bar, 200 μm.

mice with a total deficiency of PGC-1α in order to ascertain its requirement in a variety of metabolic programs. At a gross morphological level, brown adipose tissue and the brain are the only tissues that look obviously abnormal (Figures 1 and 7). Since PGC-1α has been shown to activate a broad program of gene expression in liver that recapitulates the fasted/diabetic state, and cells can be readily isolated from this tissue, we concentrated much of our initial work in liver. In isolated hepatocytes, PGC-1α is required for the execution of hormone-mediated induction of gluconeogenic gene expression. The isolated hepatocytes have a reduction in oxidative metabolism, reflecting diminished mitochondrial function. Surprisingly, the genes of gluconeogenesis are not

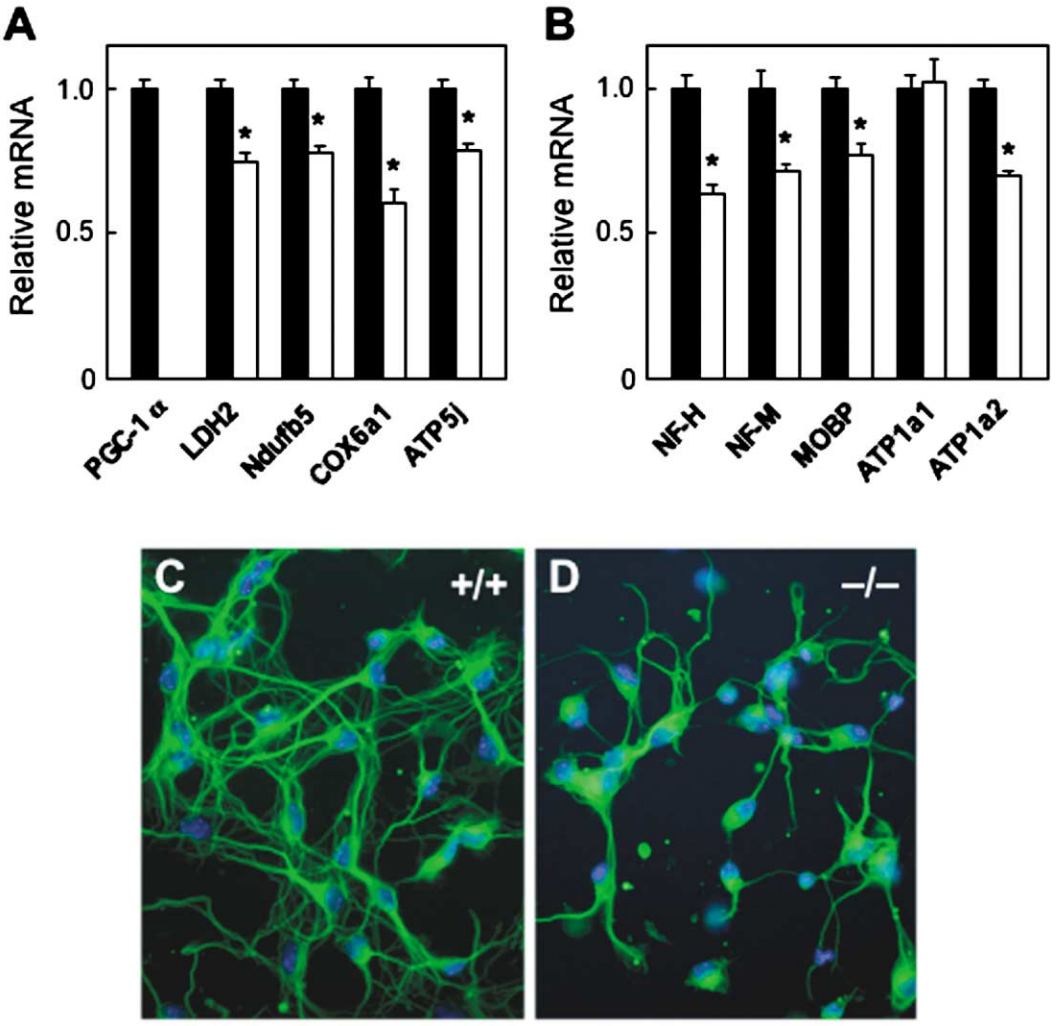

Figure 8. Gene Expression Analysis in Mouse Brain and Neurite Growth in Cultured Primary Striatal Neurons

(A) Analysis of mitochondrial gene expression in wt (filled box, n = 4) and PGC-1α-deficient (open box, n = 6) mouse brain by real-time PCR. Whole brain was dissected from 3-month-old male mice and frozen at −80°C before RNA isolation and analysis. Primers specific for *18S* ribosomal RNA were used for normalization. *$p < 0.02$.

(B) Real-time PCR analysis of nonmitochondrial genes involved in normal brain function as in (A). *$p < 0.02$.

(C and D) Wild-type and PGC-1α-deficient primary striatal neurons were cultured for 4 days and stained with a monoclonal antibody against neuron-specific class III β-tubulin and Alexa Fluor 488-labeled anti-mouse IgG antibody (Green). Nuclei were stained with DAPI in the mounting medium (blue). Note dramatically reduced neurite outgrowth in the absence of PGC-1α.

only expressed in the null mice but are locked in the "on" position; the expression of *PEPCK* and *G6Pase* is effectively uncoupled from nutritional status. Despite increased expression of mRNAs encoding gluconeogenic enzymes, mice deficient in PGC-1α have reduced hepatic gluconeogenesis in vivo. Since liver is totally dependent on the β oxidation of the fatty acids and the oxidative phosphorylation system to generate the ATP necessary for gluconeogenesis, the mild to moderate fasting hypoglycemia observed in these mice most likely occurs because of the impairment in hepatic oxidative metabolism. While this manuscript was in preparation, a study by Koo et al. showed that adenoviral-mediated expression of siRNA directed toward PGC-1α in mouse liver leads to reduced expression of gluconeogenic genes and lower hepatic glucose production (Koo et al., 2004) with no apparent compensation.

An intriguing issue here is how the null mice manage to activate the gluconeogenic genes and prevent severe hypoglycemia in the absence of PGC-1α. A survey of many of the transcription factors that have been described as being involved in this process shows one that is dysregulated in parallel with the gluconeogenic genes: C/EBPβ. We show here that C/EBPβ can potently induce *PEPCK* and *G6Pase* expression and that this activation is largely independent of PGC-1α. In fact, C/EBPβ is slightly less effective in cells lacking PGC-1α, but this does not seem to be due to a loss of coactivation of C/EBPβ by PGC-1α—PGC-1α did not coactivate C/EBPβ in standard transfection assays. More likely, the effects of PGC-1α via docking on the GR, HNF-4α, and FOXO1 are somewhat synergistic with an independent action of C/EBPβ through its own binding sites. A new model arising from these studies concerning the

dietary control of gluconeogenesis is shown in Supplemental Figure S3.

Oxidative metabolism in several tissues is reduced in mice lacking PGC-1α, but this is most apparent when the mice are given a cold challenge. As shown in Figure 5C, there is a near-total collapse of this defense against the cold, and the body temperature of PGC-1α null mice plummets, resulting in death rather quickly. Reduced mitochondrial oxidative phosphorylation in skeletal muscle has been linked with the development of insulin resistance in the elderly and in offspring of diabetic patients (Petersen et al., 2003, 2004). PGC-1α (and PGC-1β) has recently been shown to be deficient in the muscle of most Type 2 diabetes and prediabetics, suggesting a very early or even causal role in the development of this disease (Mootha et al., 2003; Patti et al., 2003). Thus, examination of the role of PGC-1α in this system is of great interest, but the very large number of other defects affecting systemic biology requires that this be done via tissue-specific ablation of *PGC-1α* in skeletal muscle. Examination and functional characterization of skeletal muscle with regard to fiber types and resistance to fatigue is under study, as is heart function.

Given these defects in oxidative metabolism, it would be expected that the PGC-1α null mice would be prone to obesity and insulin resistance, but experiments with high-fat feeding showed the exact opposite: the mice were resistant to obesity and insulin resistance. In this case, a major contributing factor seems very clear—the mice are profoundly hyperactive and have an increase in energy expenditure that correlates well with their increased activity. It is not possible to conclude that this is the complete explanation for the leanness of the null mice until possible loss of calories via urinary excretion or intestinal malabsorption is examined.

The hyperactivity and behavioral changes in the PGC-1α null mice are associated with lesions in the striatum, a brain area that plays a key role in motor coordination. In fact, previous in situ hybridization analysis revealed that PGC-1α is abundantly expressed in multiple brain areas such as the striatum, cerebral cortex, and substantia nigra in the mouse brain (Tritos et al., 2003). The prominent spongiform lesions in the striatum and, to a much less extent, in other areas of the PGC-1α null mouse brain suggest that abnormal CNS function is likely underlying the hyperactivity in the null animals. It is possible that many of these affected neurons play an inhibitory function with respect to physical movements of the mice, in that their loss is accompanied by increased movement and other neurological abnormalities.

It is rather interesting that the PGC-1α-deficient mice show a major defect in the brain. There has been a very long and extensive literature concerning mitochondrial defects and neurodegenerative diseases (Schon and Manfredi, 2003), so perhaps it is not entirely surprising that lack of PGC-1α, a major transcriptional regulator of mitochondrial function, presents with neurological defects and histological abnormalities of the brain. Genetic mutations that affect mitochondrial energy metabolism have been found to be causal in the pathogenesis of many forms of neurodegenerative diseases, such as Leigh syndrome and Friedreich ataxia (Schon and Manfredi, 2003). In addition to alterations in the expression of genes involved in oxidative metabolism and neuronal function, there is also impaired neurite growth when striatal neurons lacking PGC-1α are cultured in vitro. The spongiform lesions observed in the striatum of PGC-1α null mouse brain seem most likely due to a loss of neurites in vivo; this could reflect an impairment in energy metabolism, a problem with expression of axon-specific proteins, or both. In fact, it has been known for a long time that striatal neurons are exquisitely sensitive to impairment in oxidative metabolism, such as those caused by mitochondrial neurotoxins. The progressive nature of the striatal lesions is strongly suggested by the presence of reactive astrocytes and gliosis in the striatum of mutant mice. Neuropathological analysis on mice of different ages would provide great details as to the onset and progression of axon degeneration in affected brain areas.

While mice deficient in PGC-1α have an apparently complex neurological disorder, the striking hyperactivity with neurodegeneration is reminiscent of HD; the latter is also accompanied by a hyperkinetic movement disorder and a progressive loss of striatal neurons. In fact, patients at the earliest stages of HD typically show hyperactivity and are usually leaner than normal individuals, similar to what is shown here for the PGC-1α null mice. However, PGC-1α null mice exhibit spongiform lesions in the white matter, pathological findings not commonly seen in mouse models of HD (Mangiarini et al., 1996; Schilling et al., 1999). It is not yet known if the behavioral and movement defects shown by the PGC-1α mice are, in fact, progressive. Whether exogenous modulation of the pathways controlled by PGC-1α through genetic or pharmacological methods can improve brain function in several neurodegenerative diseases including HD also remains to be determined.

Experimental Procedures

Generation of PGC-1α Null Mice

A targeting plasmid was constructed using genomic DNA fragments derived from Sv129 mouse strain. A loxP site and a neomycin/thymidine kinase cassette flanked by two loxP sites were introduced into the PGC-1α locus. ES cell (derived from Sv129 strain) electroporation, selection, and screening were performed using standard gene targeting techniques. Briefly, genomic DNA was isolated from neomycin-resistant ES cell clones, digested with BamHI, and subjected to hybridization using probe L to detect homologous recombination and the presence of the flox allele (Supplemental Figure S1A). Chimeric founders were bred with wt C57/Bl6 mice to obtain offspring containing a germline PGC-1α flox allele. These mice were subsequently bred with ZP3-cre transgenic (in C57/Bl6 background) mice to generate *PGC-1α*$^{+/-}$ offspring. The cre recombinase-mediated generation of *PGC-1α*$^{+/-}$ allele was confirmed by Southern hybridization using probe L following restriction digestion by BamHI. Heterozygous mice were mated to obtain *PGC-1α*$^{-/-}$ mice. Genotyping of mice used in this study was performed by PCR with tail DNA as shown in Supplemental Figure S1.

Animal Experiments

All animal experiments were performed according to procedures approved by the Institutional Animal Care and Use Committee. Mice were maintained on a standard rodent chow or a high-fat diet containing 57% fat-derived calories (D12331, Research Diets) with 12 hr light and dark cycles. Plasma glucose and insulin concentrations were measured from tail blood using glucometer (Lifescan, Johnson and Johnson) and an insulin ELISA kit (Crystal Chem Inc.), respectively.

For diet-induced obesity, body weight was measured weekly for a period of 4 months. Body fat content was measured using a dual X-ray absorptiometry (Piximus, Lunar Corporation) after 3 months on the high-fat diet.

For cold exposure, 6- to 7-week-old male mice were individually housed in cages kept at 4°C with free access to food and water. Core body temperature was monitored using a rectal thermometer at various times after the start of cold exposure. Brown fat was dissected 5 hr after cold exposure and subjected to gene expression analysis.

Metabolic monitoring was performed using a Comprehensive Lab Animal Monitoring System (CLAMS, Columbia Instruments) that simultaneously measures whole-body O_2 consumption and physical movements for 16 mice. Mice were acclimated in the monitoring chambers for 2 days before the experiment to minimize the changes in housing environments. Data was collected every 48 min for each mouse over a period of 3 days. Metabolic rate and physical activity were averaged for the whole study period with the exception of the first five data points that tend to be influenced by animal handling at the beginning of studies.

Histological Analysis

Tissues were dissected and fixed in 4% paraformaldehyde overnight and rinsed with phosphate-buffered saline. Brown fat was subsequently dehydrated and embedded in plastic (JB-4, Electron Microscopy Sciences) and sectioned at 1.5 μm for H&E staining. Liver was dehydrated in ethanol, paraffin embedded, and sectioned at 4 μm for H&E staining.

Brain tissue for neuropathological examination was prepared from 6- and 12-week-old wt and PGC-1α null mice. Tissues were fixed in situ by intracardiac perfusion with 15 ml PBS followed by 30 ml 4% PFA in PBS. Brains were removed, postfixed in 4% PFA overnight at 4°C, and embedded in paraffin. Coronal sections (6 μm) were stained both conventionally, with H&E, Luxol fast blue (H&E + LFB), and 0.1% cresyl echt violet (Nissl), and immunohistochemically, with antibodies against glial fibrillary acidic protein (GFAP, polyclonal antibody 1:200; Dako, Hamburg, Germany) as an astrocyte marker and against neurofilament 200 kDa (monoclonal antibody 1:50; Sigma) to label axons.

RNA and Protein Analysis

Total RNA was isolated from cultured hepatocytes or tissues using Trizol reagents (Invitrogen). For hybridization, 10–20 μg of RNA samples were separated on a formaldehyde gel, transferred to nylon membrane, and then hybridized with gene-specific probes. For real-time PCR analysis, RNA samples were reverse transcribed and used in quantitative PCR reactions in the presence of a fluorescent dye (Cybergreen, Bio-Rad). Relative abundance of mRNA was calculated after normalization to *18S* ribosomal RNA. Sequences for the primers used in this study were shown in Supplemental Table S4.

For the detection of PGC-1α protein, nuclear extracts (80 μg) prepared from brown fat were analyzed by immunoblotting using mouse polyclonal antibodies raised against the purified C terminus of PGC-1α. Muscle AMPK was detected with antibodies that recognize total AMPK (#07–181, Upstate Biotechnology) or phosphorylated AMPK (2531, Cell Signaling Technology). ACC phosphorylation was detected using a phospho-ACC-specific antibody (3661, Cell Signaling Technology).

Primary Hepatocytes

Primary hepatocytes were isolated following perfusion of whole liver first with perfusion buffer (Hank's Balanced Saline, HBSS) and then with collagenase solution (HBSS with 1% BSA and 0.05% collagenase) for 10 min. Dispersed cells were resuspended and seeded onto collagen-coated plates in DMEM supplemented with 10% fetal bovine serum in the presence of 1 mM sodium pyruvate, 1 μM dexamethasone (Dex), and 50 nM insulin. Two hours after plating, the medium was changed to a maintenance medium containing DMEM supplemented with 0.1% BSA and 1 mM sodium pyruvate. For hormonal treatments, hepatocytes were cultured in minimal media (DMEM with 0.1% BSA) for 40 hr and then treated with 0.2 μM or 1 μM of a combination of forskolin and Dex for 3 or 6 hr before RNA isolation.

For adenoviral infection, hepatocytes were incubated with varying titers of adenovirus expressing either GFP or C/EBPβ for 3 hr and then maintained in starvation media for 24 hr. Infected cells were treated with 0.2 μM forskolin and 0.1 μM Dex for 3 hr before RNA isolation.

For respiration measurements, hepatocytes were cultured in the presence of 0.2 μM Dex overnight and then removed from plates by incubating with the trypsin/EDTA solution. O_2 consumption was measured essentially as previously described (Fan et al., 2004; Wu et al., 1999). Measurements were performed in the presence of 25 mM glucose, 1 mM pyruvate, and 2% BSA.

Insulin/Glucose/Pyruvate Tolerance Tests

For the insulin tolerance test, high-fat-fed mice were fasted for 4 hr before receiving an intraperitoneal injection of insulin at 0.8 mU/kg. Plasma glucose levels were measured from tail blood before or 15, 30, 45, 60, and 100 min after insulin infusion.

For the glucose tolerance test, high-fat-fed mice were fasted overnight (14 hr) and injected intraperitoneally with a glucose solution (prepared in saline) at 2 g/kg. Plasma glucose levels were measured from tail blood before or 15, 30, 45, 60, 90, and 180 min after glucose infusion.

The pyruvate tolerance test was performed as described (Miyake et al., 2002). Briefly, 3-month-old male mice were fasted for 14 hr before receiving an intraperitoneal dose of pyruvate (in saline) at 2 g/kg. Plasma glucose levels were determined as indicated above.

Transient Transfection

Mouse H2.35 hepatoma cells (CRL-1995, ATCC) were maintained in DMEM supplemented with 4% fetal bovine serum in the presence of 0.2 μM dex. For transfection, 100 ng of reporter plasmid (Gal-C/EBPβ) was transiently transfected using Superfect (Qiagen) in the presence of 500 ng of vector or pcDNA3-PGC-1α. Luciferase activity was measured 40 hr following transfection.

Acknowledgments

We thank Drs. Eric Bachman and Pere Puigserver for comments and critiques on the manuscript. We also thank Dr. P. Reed Larsen for T3 antibody; Eric Smith for computer graphics support; and Jia Yu and Mingtao Lee for technical assistance in ES cell manipulations and CLAMS studies, respectively. This work is supported by grants from the N.I.H., DK54477 and DK61562 (B.M.S.), DK40936 (G.I.S.), NS002174 and NS045242 (D.K.) and DK065584 (J.L.), and QLK1-2001-00183 DLARFID (S.C.).

Received: May 14, 2004
Revised: August 4, 2004
Accepted: August 17, 2004
Published: September 30, 2004

References

Aoki, T.T. (1981). Metabolic adaptations to starvation, semistarvation, and carbohydrate restriction. Prog. Clin. Biol. Res. *67*, 161–177.

Baar, K., Wende, A.R., Jones, T.E., Marison, M., Nolte, L.A., Chen, M., Kelly, D.P., and Holloszy, J.O. (2002). Adaptations of skeletal muscle to exercise: rapid increase in the transcriptional coactivator PGC-1. FASEB J. *16*, 1879–1886.

Bouillaud, F., Ricquier, D., Thibault, J., and Weissenbach, J. (1985). Molecular approach to thermogenesis in brown adipose tissue: cDNA cloning of the mitochondrial uncoupling protein. Proc. Natl. Acad. Sci. USA *82*, 445–448.

Carling, D. (2004). The AMP-activated protein kinase cascade—a unifying system for energy control. Trends Biochem. Sci. *29*, 18–24.

Croniger, C., Trus, M., Lysek-Stupp, K., Cohen, H., Liu, Y., Darlington, G.J., Poli, V., Hanson, R.W., and Reshef, L. (1997). Role of the isoforms of CCAAT/enhancer-binding protein in the initiation of phosphoenolpyruvate carboxykinase (GTP) gene transcription at birth. J. Biol. Chem. *272*, 26306–26312.

Croniger, C., Leahy, P., Reshef, L., and Hanson, R.W. (1998). C/EBP

and the control of phosphoenolpyruvate carboxykinase gene transcription in the liver. J. Biol. Chem. *273*, 31629–31632.

Fan, M., Rhee, J., St-Pierre, J., Handschin, C., Puigserver, P., Lin, J., Jaeger, S., Erdjument-Bromage, H., Tempst, P., and Spiegelman, B.M. (2004). Suppression of mitochondrial respiration through recruitment of p160 myb binding protein to PGC-1alpha: modulation by p38 MAPK. Genes Dev. *18*, 278–289.

Ginsberg, H.N. (2000). Insulin resistance and cardiovascular disease. J. Clin. Invest. *106*, 453–458.

Goto, M., Terada, S., Kato, M., Katoh, M., Yokozeki, T., Tabata, I., and Shimokawa, T. (2000). cDNA Cloning and mRNA analysis of PGC-1 in epitrochlearis muscle in swimming-exercised rats. Biochem. Biophys. Res. Commun. *274*, 350–354.

Hanson, R.W., and Reshef, L. (1997). Regulation of phosphoenolpyruvate carboxykinase (GTP) gene expression. Annu. Rev. Biochem. *66*, 581–611.

Herzig, S., Long, F., Jhala, U.S., Hedrick, S., Quinn, R., Bauer, A., Rudolph, D., Schutz, G., Yoon, C., Puigserver, P., et al. (2001). CREB regulates hepatic gluconeogenesis through the coactivator PGC-1. Nature *413*, 179–183.

Horton, J.D., Goldstein, J.L., and Brown, M.S. (2002). SREBPs: activators of the complete program of cholesterol and fatty acid synthesis in the liver. J. Clin. Invest. *109*, 1125–1131.

Jacobsson, A., Stadler, U., Glotzer, M.A., and Kozak, L.P. (1985). Mitochondrial uncoupling protein from mouse brown fat. Molecular cloning, genetic mapping, and mRNA expression. J. Biol. Chem. *260*, 16250–16254.

Kelly, D.P., and Scarpulla, R.C. (2004). Transcriptional regulatory circuits controlling mitochondrial biogenesis and function. Genes Dev. *18*, 357–368.

Kirpichnikov, D., McFarlane, S.I., and Sowers, J.R. (2002). Metformin: an update. Ann. Intern. Med. *137*, 25–33.

Koo, S.H., Satoh, H., Herzig, S., Lee, C.H., Hedrick, S., Kulkarni, R., Evans, R.M., Olefsky, J., and Montminy, M. (2004). PGC-1 promotes insulin resistance in liver through PPAR-alpha-dependent induction of TRB-3. Nat. Med. *10*, 530–534.

Lehman, J.J., Barger, P.M., Kovacs, A., Saffitz, J.E., Medeiros, D.M., and Kelly, D.P. (2000). Peroxisome proliferator-activated receptor gamma coactivator-1 promotes cardiac mitochondrial biogenesis. J. Clin. Invest. *106*, 847–856.

Lewandoski, M., Wassarman, K.M., and Martin, G.R. (1997). Zp3-cre, a transgenic mouse line for the activation or inactivation of loxP-flanked target genes specifically in the female germ line. Curr. Biol. *7*, 148–151.

Lieberman, L.S. (2003). Dietary, evolutionary, and modernizing influences on the prevalence of type 2 diabetes. Annu. Rev. Nutr. *23*, 345–377.

Lin, J., Puigserver, P., Donovan, J., Tarr, P., and Spiegelman, B.M. (2002a). Peroxisome proliferator-activated receptor gamma coactivator 1beta (PGC-1beta), a novel PGC-1-related transcription coactivator associated with host cell factor. J. Biol. Chem. *277*, 1645–1648.

Lin, J., Wu, H., Tarr, P.T., Zhang, C.Y., Wu, Z., Boss, O., Michael, L.F., Puigserver, P., Isotani, E., Olson, E.N., et al. (2002b). Transcriptional co-activator PGC-1 alpha drives the formation of slow-twitch muscle fibres. Nature *418*, 797–801.

Lin, J., Tarr, P.T., Yang, R., Rhee, J., Puigserver, P., Newgard, C.B., and Spiegelman, B.M. (2003). PGC-1beta in the regulation of hepatic glucose and energy metabolism. J. Biol. Chem. *278*, 30843–30848.

Liu, S., Croniger, C., Arizmendi, C., Harada-Shiba, M., Ren, J., Poli, V., Hanson, R.W., and Friedman, J.E. (1999). Hypoglycemia and impaired hepatic glucose production in mice with a deletion of the C/EBPbeta gene. J. Clin. Invest. *103*, 207–213.

Mangiarini, L., Sathasivam, K., Seller, M., Cozens, B., Harper, A., Hetherington, C., Lawton, M., Trottier, Y., Lehrach, H., Davies, S.W., and Bates, G.P. (1996). Exon 1 of the HD gene with an expanded CAG repeat is sufficient to cause a progressive neurological phenotype in transgenic mice. Cell *87*, 493–506.

Miyake, K., Ogawa, W., Matsumoto, M., Nakamura, T., Sakaue, H., and Kasuga, M. (2002). Hyperinsulinemia, glucose intolerance, and dyslipidemia induced by acute inhibition of phosphoinositide 3-kinase signaling in the liver. J. Clin. Invest. *110*, 1483–1491.

Moller, D.E. (2001). New drug targets for type 2 diabetes and the metabolic syndrome. Nature *414*, 821–827.

Mootha, V.K., Lindgren, C.M., Eriksson, K.F., Subramanian, A., Sihag, S., Lehar, J., Puigserver, P., Carlsson, E., Ridderstrale, M., Laurila, E., et al. (2003). PGC-1alpha-responsive genes involved in oxidative phosphorylation are coordinately downregulated in human diabetes. Nat. Genet. *34*, 267–273.

Nordlie, R.C., Foster, J.D., and Lange, A.J. (1999). Regulation of glucose production by the liver. Annu. Rev. Nutr. *19*, 379–406.

Park, E.A., Gurney, A.L., Nizielski, S.E., Hakimi, P., Cao, Z., Moorman, A., and Hanson, R.W. (1993). Relative roles of CCAAT/enhancer-binding protein beta and cAMP regulatory element-binding protein in controlling transcription of the gene for phosphoenolpyruvate carboxykinase (GTP). J. Biol. Chem. *268*, 613–619.

Patti, M.E., Butte, A.J., Crunkhorn, S., Cusi, K., Berria, R., Kashyap, S., Miyazaki, Y., Kohane, I., Costello, M., Saccone, R., et al. (2003). Coordinated reduction of genes of oxidative metabolism in humans with insulin resistance and diabetes: potential role of PGC1 and NRF1. Proc. Natl. Acad. Sci. USA *100*, 8466–8471.

Petersen, K.F., Befroy, D., Dufour, S., Dziura, J., Ariyan, C., Rothman, D.L., DiPietro, L., Cline, G.W., and Shulman, G.I. (2003). Mitochondrial dysfunction in the elderly: possible role in insulin resistance. Science *300*, 1140–1142.

Petersen, K.F., Dufour, S., Befroy, D., Garcia, R., and Shulman, G.I. (2004). Impaired mitochondrial activity in the insulin-resistant offspring of patients with type 2 diabetes. N. Engl. J. Med. *350*, 664–671.

Pilkis, S.J., and Granner, D.K. (1992). Molecular physiology of the regulation of hepatic gluconeogenesis and glycolysis. Annu. Rev. Physiol. *54*, 885–909.

Puigserver, P., Wu, Z., Park, C.W., Graves, R., Wright, M., and Spiegelman, B.M. (1998). A cold-inducible coactivator of nuclear receptors linked to adaptive thermogenesis. Cell *92*, 829–839.

Puigserver, P., and Spiegelman, B.M. (2003). Peroxisome proliferator-activated receptor-gamma coactivator 1 alpha (PGC-1 alpha): transcriptional coactivator and metabolic regulator. Endocr. Rev. *24*, 78–90.

Rhee, J., Inoue, Y., Yoon, J.C., Puigserver, P., Fan, M., Gonzalez, F.J., and Spiegelman, B.M. (2003). Regulation of hepatic fasting response by PPARgamma coactivator-1alpha (PGC-1): requirement for hepatocyte nuclear factor 4alpha in gluconeogenesis. Proc. Natl. Acad. Sci. USA *100*, 4012–4017.

Roesler, W.J. (2001). The role of C/EBP in nutrient and hormonal regulation of gene expression. Annu. Rev. Nutr. *21*, 141–165.

Saltiel, A.R., and Kahn, C.R. (2001). Insulin signalling and the regulation of glucose and lipid metabolism. Nature *414*, 799–806.

Schilling, G., Becher, M.W., Sharp, A.H., Jinnah, H.A., Duan, K., Kotzuk, J.A., Slunt, H.H., Ratovitski, T., Cooper, J.K., Jenkins, N.A., et al. (1999). Intranuclear inclusions and neuritic aggregates in transgenic mice expressing a mutant N-terminal fragment of huntingtin. Hum. Mol. Genet. *8*, 397–407.

Schon, E.A., and Manfredi, G. (2003). Neuronal degeneration and mitochondrial dysfunction. J. Clin. Invest. *111*, 303–312.

Shin, D.J., Campos, J.A., Gil, G., and Osborne, T.F. (2003). PGC-1alpha activates CYP7A1 and bile acid biosynthesis. J. Biol. Chem. *278*, 50047–50052.

St-Pierre, J., Lin, J., Krauss, S., Tarr, P.T., Yang, R., Newgard, C.B., and Spiegelman, B.M. (2003). Bioenergetic analysis of peroxisome proliferator-activated receptor gamma coactivators 1alpha and 1beta (PGC-1alpha and PGC-1beta) in muscle cells. J. Biol. Chem. *278*, 26597–26603.

Tritos, N.A., Mastaitis, J.W., Kokkotou, E.G., Puigserver, P., Spiegelman, B.M., and Maratos-Flier, E. (2003). Characterization of the peroxisome proliferator activated receptor coactivator 1 alpha (PGC 1alpha) expression in the murine brain. Brain Res. *961*, 255–260.

Wu, Z., Puigserver, P., Andersson, U., Zhang, C., Adelmant, G., Mootha, V., Troy, A., Cinti, S., Lowell, B., Scarpulla, R.C., and Spiegelman, B.M. (1999). Mechanisms controlling mitochondrial biogenesis and respiration through the thermogenic coactivator PGC-1. Cell *98*, 115–124.

Yoon, J.C., Puigserver, P., Chen, G., Donovan, J., Wu, Z., Rhee, J., Adelmant, G., Stafford, J., Kahn, C.R., Granner, D.K., et al. (2001). Control of hepatic gluconeogenesis through the transcriptional coactivator PGC-1. Nature *413*, 131–138.

Zimmet, P., Alberti, K.G., and Shaw, J. (2001). Global and societal implications of the diabetes epidemic. Nature *414*, 782–787.